Check for updates

Water Practice & Technology

IWA PUBLISHING

© 2024 The Authors

Water Practice & Technology Vol 19 No 8, 3317 doi: 10.2166/wpt.2024.184

Photocatalytic degradation of methyl orange and methyl violet dyes by UV/Cu^{2+}/PDS process

Adnan Ali[a], Qaiser Khan[a], Faiza Rehman[b], Ikhtiar Gul[a], Faryal Gohar[a], Muhammad Zohaib[a] and Murtaza Sayed[a,*]

[a] Radiation and Environmental Chemistry Laboratory, National Centre of Excellence in Physical Chemistry, University of Peshawar, Peshawar, 25120, Pakistan
[b] Department of Chemistry, University of Poonch, Rawalakot, Azad Kashmir, Pakistan
*Corresponding author. E-mail: murtazasayed@uop.edu.pk

MS, 0000-0002-2194-8058

ABSTRACT

This research is focused on the application of the UV/Cu^{2+}/peroxydisulfate (PDS) system for the successful decolorization of methyl orange (MO) and methyl violet (MV) dyes in aqueous media. The effects of different parameters such as the equilibrium time, initial catalyst amount, PDS concentration and pH of the media in terms of MO and MV degradation were studied. Furthermore, the photocatalytic performance of the UV/Cu^{2+}/PDS system was also investigated by performing the degradation of MO and MV in different water systems including distilled water, synthetic wastewater and industrial wastewater samples. The results revealed 94 and 89% degradation for MO and MV dyes in the UV/Cu^{2+}/PDS system, respectively. The radical quenching experiments showed sulfate radicals ($SO_4^{\cdot-}$) as the prominent species involved in the degradation of MO and MV dyes. Overall, it was concluded that the UV/Cu^{2+}/PDS process has the ability to be adopted for the effective elimination of contaminants from the aquatic system.

Key words: advanced oxidation processes (AOPs), degradation, methyl orange and methyl violet, peroxydisulfate, photocatalysis, textile dyes

HIGHLIGHTS

- A novel UV/Cu^{2+}/PDS process was developed for the efficient removal of MO and MV dyes from aqueous media.
- The effects of various operational parameters in the degradation of the selected contaminants were studied.
- Sulfate radicals were the dominant species in the contaminant degradation.

GRAPHICAL ABSTRACT

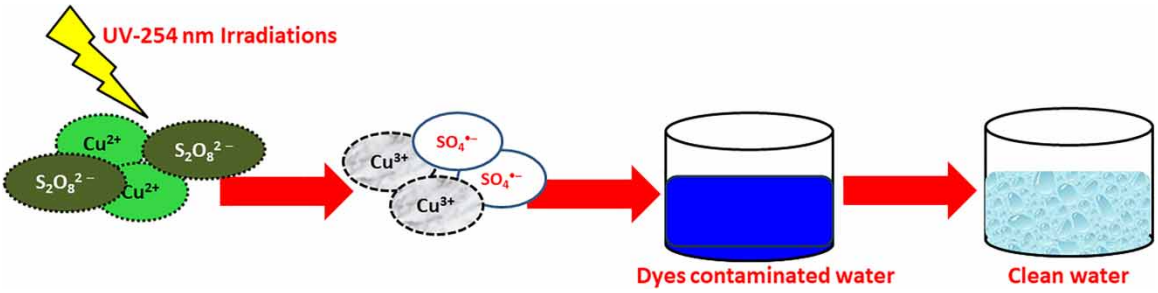

1. INTRODUCTION

Water is one of the most significant components of the planet Earth. Water covers approximately 71% of the earth's surface (El-Regal & Satheesh 2023). To survive, all plants and animals require water in their bodies. Water is used for plenty of purposes, including drinking, bathing, washing, cooking, cleaning, and plantation, and in industries for various industrial practices and the production of various commercial products (Inyinbor Adejumoke *et al.* 2018). Different anthropogenic activities play a major role in water contamination. Among

This is an Open Access article distributed under the terms of the Creative Commons Attribution Licence (CC BY 4.0), which permits copying, adaptation and redistribution, provided the original work is properly cited (http://creativecommons.org/licenses/by/4.0/).

Downloaded from http://iwaponline.com/wpt/article-pdf/19/8/3317/1472464/wpt2024184.pdf
by guest

these, industries play a major role by releasing massive quantities of hazardous materials, including dyes, antibiotics, and pesticides, either directly or indirectly into the aquatic environment and polluting it (Kuchangi *et al.* 2023). Textile industries contribute significantly to water pollution due to the release of various dyes into aquatic systems (Sidabutar *et al.* 2017). According to the literature, 10–20% of dyes are lost to wastewater due to inefficient operation in the dyeing process. The dye-contaminated wastewater inhibits the reoxygenation capacity of water, cuts off sunlight and disrupts biological activity in aquatic life (Zaharia *et al.* 2009).

The most intriguing of these dyes is methyl orange (MO, $C_{14}H_{14}N_3NaO_3S$), an azo-anionic dye soluble in water. MO turns red in acidic and yellow in basic media. Because of its clear and distinct color variation at different pH media, MO is used as an indicator in the titration process (Al-Mamun *et al.* 2021). Another most important dye is methyl violet (MV, $C_{24}H_{28}N_3Cl$), a cationic dye that belongs to the aromatic organic compounds family. It gives yellow color at low pH (0.15) and changes to violet as the pH increases. As MV is a mutagen and mitotic poison, there are concerns about the environmental impact because of its release into the freshwater body (Thekkedath *et al.* 2022). These dyes (MO and MV) are persistent in nature, non-biodegradable and highly soluble in water; therefore, their removal from the aquatic system is of high concern (Shah 2023). Due to their persistent and non-biodegradable nature, these dyes cannot be easily eliminated from aquatic bodies by traditional wastewater treatment procedures.

Different types of efficient advanced oxidation processes (AOPs) have been widely investigated, such as Fenton processes, UV-photolysis-driven processes, ozonation and sulfate radical-based AOPs (SR-AOPs), for the removal of dyes from wastewater (Liu *et al.* 2023b; Khan *et al.* 2024). The UV-based photocatalytic processes are also well documented for the production of hydrogen energy as a clean energy (Orak & Yüksel 2021; Orak & Yüksel 2022a, 2022b; Keskin *et al.* 2024). In addition, various oxidants such as peroxymonosulfate and peroxydisulfate (PDS) were broadly accepted in recent years in both research and application for the remediation of organic pollutants in wastewater (Liu *et al.* 2023a). Activation of these oxidants through alkaline medium, UV, heat and transition metals can produce strong sulfate radicals ($SO_4^{\cdot-}$) that cause contaminants degradation in aqueous media (Zhang *et al.* 2014). Among the said processes, SR-AOP is the most efficient way the treatment of dye-contaminated wastewater.

Chakma *et al.* (2017) used sono-hybrid techniques (US/Fe^{2+}/UVC) for the activation of persulfate (PS). The efficiency of the system was determined in terms of azorubine degradation in aqueous media. The results revealed that US/UVC/PS is the best technique for the degradation of azorubine in water. The incorporation of Fe^{2+} in the US/UVC/PS system decreased the efficiency of the processes because of the scavenging of $SO_4^{\cdot-}$ by Fe^{2+} ions in aqueous media. Bougdour *et al.* (2020) used the PDS/Fe(II)/UV technique for the elimination of RY17, RR120 and RB19 dyes in synthetic wastewater (SW) and real water samples. Under optimum conditions ([PDS] = 1 mM, $T = 25$ °C), 96.1, 99.2 and 100% degradation were observed for RY17, RR120 and RB19, respectively, in 2 h of reaction time. Moreover, about 80% mineralization of the mixture of these three dyes (RY17, RR120 and RB19) was observed at a treatment time of 2 h in an SW sample. In addition, the real waste sample showed 66% degradation of the selected contaminants under the same conditions.

The present study is aimed at the degradation of MO and MV dyes in aqueous media using a UV/Cu^{2+}/PDS system. The influences of different operational factors such as initial contaminant concentration, initial amount of catalyst and oxidant and initial solution pH toward contaminants degradation were also examined. The efficiency of the UV/Cu^{2+}/PDS system was also determined in different water systems including distilled water (DW), SW and industrial wastewater (IW) samples. Furthermore, scavenger experiments were also carried out to determine the active species responsible for the degradation of the selected contaminants.

2. MATERIALS AND METHODS

2.1. Materials

MO ($C_{14}H_{14}N_3NaO_3S$, 99%), MV ($C_{24}H_{28}N_3Cl$, 84%), sodium hydroxide (NaOH), perchloric acid ($HClO_4$), methanol (CH_3OH, 99.85%) and isopropyl alcohol $(CH_3)_2CHOH$, 99.5%) were provided by Sigma Aldrich. Tertiary butanol ($C_4H_{10}O$, 99.65%), copper (II) chloride ($CuCl_2.2H_2O$, 98%) and sodium PDS ($Na_2S_2O_8$, 98%) were purchased from Scharlau Spain.

2.2. Methods

2.2.1. Preparation and calibration of dyes solutions

Before performing the photolysis and photocatalysis experiments, the calibration plots were drawn for MO and MV dyes, respectively. Figures 1 and 2 show the corresponding calibration curves for MO and MV dyes. These

Downloaded from http://iwaponline.com/wpt/article-pdf/19/8/3317/1472464/wpt2024184.pdf
by guest

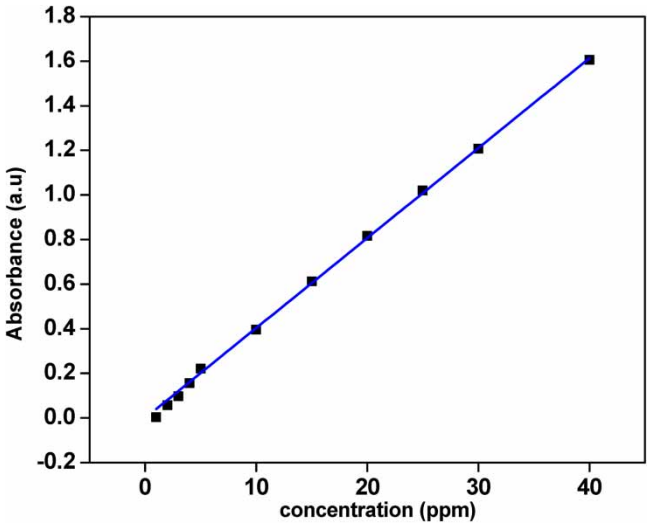

Figure 1 | Calibration curve for MO dye. Experimental conditions: [MO] = 1–40 ppm, pH_{MO} = 4.5, radiation source = UV (15 W).

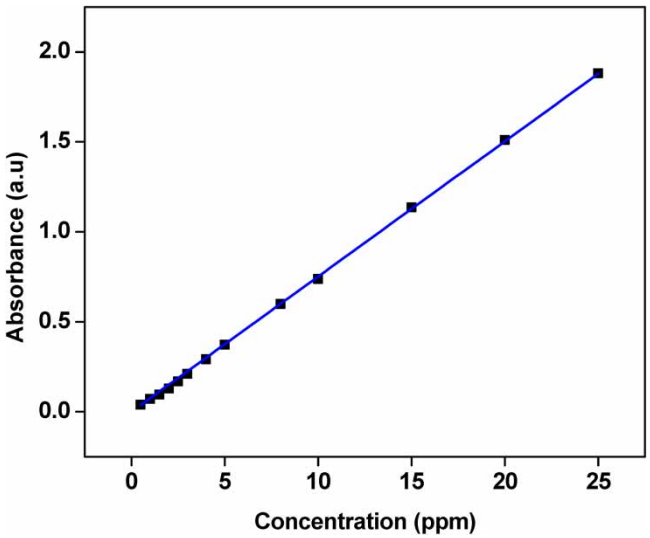

Figure 2 | Calibration curve for MV dye. Experimental conditions: [MV] = 0.5–25 ppm, pH_{MV} = 5.6, radiation source = UV lamp (15 W).

curves showed that absorbance regularly increases with increasing the initial concentration of MO and MV dyes hence obeying the Beer–Lambert law.

2.2.2. Photocatalytic reactor setup and photocatalytic procedures

A 150 mL Petri dish was used for performing the degradation experiments. The Petri dish was placed under the UV light source, ensuring that the entire solution was exposed to UV radiation. The magnetic stirrer was set up inside the reaction mixture in a Petri dish to maintain uniform mixing during the degradation process. The photocatalytic setup for the degradation of the MO and MV dyes was carried out under a 15 W UV lamp, placed in a wooden chamber.

2.2.3. Photocatalytic degradation of MO and MV dyes

The UV light source (mercury lamp, 15 W) was turned on and adjusted the intensity according to the experimental requirements. The magnetic stirrer was turned on to ensure continuous mixing of the solution. The reaction progress was monitored by collecting samples at regular time intervals. The first sample was collected in the initial stage when the lamp was off regarded as 0 min and last at 40 min, which showed maximum degradation.

Downloaded from http://iwaponline.com/wpt/article-pdf/19/8/3317/1472464/wpt2024184.pdf
by guest

The absorbance of dye solutions was measured using SpectroVis Plus, Vernier, USA. The absorbance wavelength for MO and MV was measured at 515 and 588 nm, respectively. From the absorbance data, the final concentration (C_f) was calculated. Similarly, by using the degradation formula, the percent degradation after each interval of time was obtained (Equation (1)).

$$\% \text{ Degradation} = \frac{C_0 - C_f}{C_0} \times 100 \quad (1)$$

where C_0 represents the initial concentration of the contaminants (MO and MV), while C_f is the concentration of contaminants at time t (Khan *et al.* 2023). Table 1 represents the photocatalytic degradation of MO and MV dyes by other researchers in identical experimental conditions.

Table 1 | Comparisons of various photocatalytic/catalytic processes for the degradation of MO and/or MV dyes

S. No.	Photocatalytic system	Dye Name	% degradation	Irradiation time (min)	Ref.
1	Activated carbon (AC) supported sulphur-based Ni/Co photocatalysts	MV	98	90	Artagan *et al.* (2021)
2	CuS/Fe_3O_4 for activation of PS	MO	94	30	Zhang *et al.* (2023)
3	Pyrite (FeS2)-activated PS	MO	92.9	150	Liu *et al.* (2022)
4	Visible light activation of PS (2 mM) using tris(2,2′-bipyridyl)ruthenium(ii)	MO	98	12	Gokulakrishnan *et al.* (2013)
5	CuFe-layered double hydroxide (CuFe-LDH) to activate PDS	MV	100	18	Tian *et al.* (2022)
6	UV/Cu^{2+}/PDS process	MO MV	94 89	40 40	This study

2.2.4. Analysis of degradation byproducts

The analysis of degradation byproducts (DPs) of MO and MV was done using gas chromatography coupled mass spectrometry (GC-MS) QP 2010 plus (Shimadzu, Japan) installed with a DB-5MS column (30 m × 0.25 mm × 0.25 m). The DPs of MO and MV were analyzed for the m/z values in the range of 40–800. The analytical conditions of GC were injection temperature = 240 °C and oven temperature was first set at 40 °C and then was increased to 280 °C at the ramping rate of 4 °C/min. For GC-MS analysis, the DPs of MO and MV were extracted in methanol by the solvent extraction technique. The details of the GC-MS procedure are documented in our earlier publication (Zohaib *et al.* 2024).

2.2.5. Optimization and control experiments

Control experiments were conducted without Cu^{2+} ions and/or PDS to evaluate the contribution of each component to the degradation process. Optimization experiments were performed by varying parameters such as reaction time, initial concentration of Cu^{2+} ions and PDS to determine the optimal condition for efficient degradation. Moreover, the degradation of MO and MV was also performed in distilled, SW and IW samples to determine the efficiency of the UV/Cu^{2+}/PDS system.

3. RESULTS AND DISCUSSION

3.1. Photolysis of MO and MV

Prior to photocatalysis, the photolysis of MO and MV dyes was performed to determine the stability of these dyes under UV irradiations. The results of photolysis experiments are depicted in Figure 3. It can be seen from Figure 3 that continuous exposure for 40 min under UV irradiations cause only 1.94 and 10.92% degradation for MO and MV dyes with the corresponding k_{app} values of 5.00×10^{-4} and 2.30×10^{-3} min^{-1}, respectively. The low percent degradation of both MO (1.94%) and MV (10.92%) dyes in UV alone could be attributed to their molecular structure and chemical stability (Rehman *et al.* 2018). The results of the photolysis confirmed the stability of these dyes under UV irradiations.

Downloaded from http://iwaponline.com/wpt/article-pdf/19/8/3317/1472464/wpt2024184.pdf
by guest

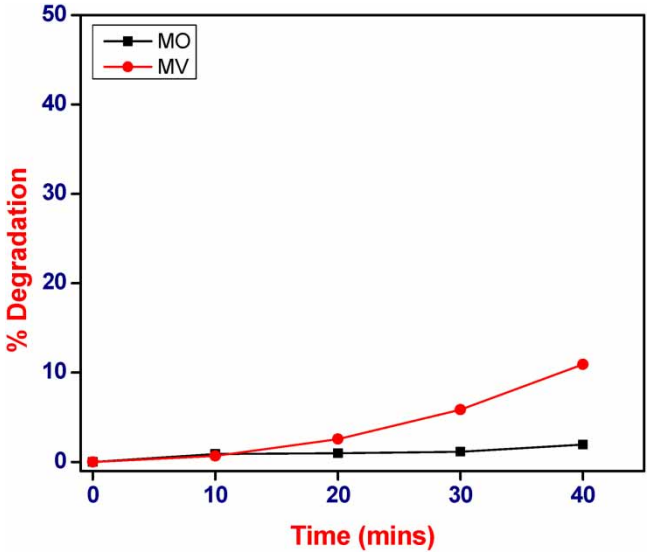

Figure 3 | Photocatalytic degradation of MO and MV dyes under UV irradiations. Experimental conditions: $[MO]_0 = 10$ ppm; $[MV]_0 = 25$ ppm; radiation source = UV lamp (15 W); radiation time = 40 min, $pH_{MO} = 4.5$, $pH_{MV} = 5.6$.

3.2. Initial PDS concentration on the degradation of MO and MV by UV/PDS process

Sodium peroxydisulfate or simply sodium persulfate (NaS_2O_8) was the active source utilized for the production of sulfate radicals ($SO_4^{\cdot-}$). When exposed to light, PDS acts as an oxidizing agent that leads to the formation of highly reactive sulfate radicals ($SO_4^{\cdot-}$) (Equation (2)) (Nidheesh *et al.* 2022). The generated sulfate radicals attack the dye molecules (MO and MV) and cause their elimination from aqueous media. The removal of electron-rich functional groups from the dye molecule is frequently involved in this process, which results in the formation of simpler, colorless compounds (Ismail & Sakai 2022).

Figure 4 shows the degradation of MO and MV dyes using the UV/PDS system. The results indicated that increasing the initial PDS concentration from 0.5 to 1.5 mM, the increase in percent degradation from 57.3 to 79.4% for MO and from 59.7 to 61% for MV dyes, respectively, was achieved. However, further increasing the PDS concentration from 1.5 mM to 2.0, 2.5 and 3 mM caused a decrease in percent degradation for these contaminants to 74.2, 70.3 and 66% for MO and 70.3, 67.0 and 61.0% for MV, respectively. It is due to the fact that at the lower concentration of PDS, a lower rate of OH is generated, which increases as the initial

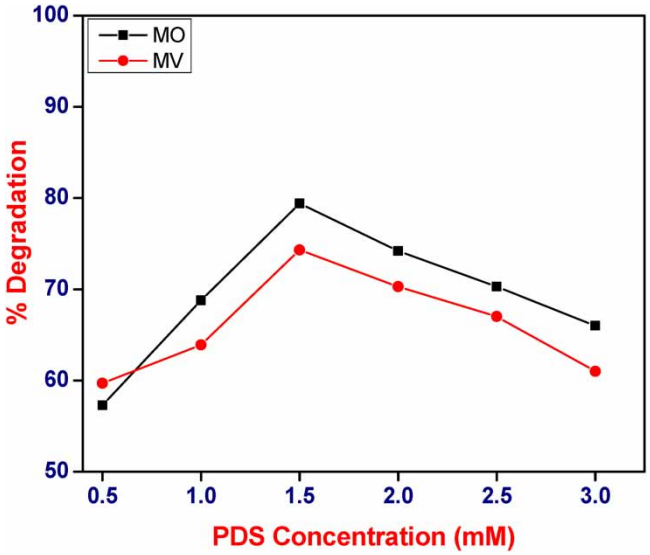

Figure 4 | Degradation of MO and MV dyes by PDS under UV irradiations. Experimental conditions: $[MO]_0 = 10$ ppm; $[MV]_0 = 25$ ppm, radiation source = UV lamp (15 W); [PDS] concentration (0.5–3 mM), radiation time = 40 min, $pH_{MO} = 4.5$, $pH_{MV} = 5.6$.

Downloaded from http://iwaponline.com/wpt/article-pdf/19/8/3317/1472464/wpt2024184.pdf
by guest

concentration of PDS increases. The decrease in percent degradation after increasing the PDS concentration beyond 1.5 mM could be associated with the decrease in the efficiency of the PDS system due to the formation of less reactive side species. For example, the excess amount of PDS reacts with the available $SO_4^{\cdot-}$ in the solution resulting in the formation of less reactive $S_2O_8^{\cdot-}$ (as shown by Equation (3)) (Bekkouche *et al.* 2017; Nidheesh *et al.* 2022). In addition, the radical–radical recombination phenomena are also expected at higher PDS doses as shown by Equation (4) (Bekkouche *et al.* 2017). Thus, a PDS concentration of 1.5 mM is the optimized concentration.

$$S_2O_8^{2-} \xrightarrow{\text{light}} 2SO_4^{\cdot-} \tag{2}$$

$$SO_4^{\cdot-} + S_2O_8^{2-} \rightarrow S_2O_8^{\cdot-} + SO_4^{2-} \qquad k = 6.1 \times 10^5 M^{-1}s^{-1} \tag{3}$$

$$SO_4^{\cdot-} + SO_4^{\cdot-} \rightarrow S_2O_8^{2-} \qquad k = 4 \times 10^8 M^{-1}s^{-1} \tag{4}$$

These results are in agreement with the study conducted by Badi *et al.* (2019) where the degradation performance was reduced for the degradation of dimethyl phthalate when the PS concentration was further increased from the optimum amount. The results of Pasalari *et al.* (2022) are also inconsistent with these results where the photocatalytic degradation of 2,4-dinitrophenol was significantly reduced when PS concentration was increased to 100 mg L^{-1}.

3.3. Initial Cu^{2+} concentration on the photocatalytic degradation of MO and MV by UV/Cu^{2+}/PDS process

Once the optimum concentration of PDS (1.5 mM) was achieved, then the next experiment was carried out using various initial concentrations of Cu^{2+} ions in combination with PDS (1.5 mM). The concentration of PDS 1.5 mM was taken constantly while the concentration of Cu^{2+} varied from 0.5 to 3 mM.

Figure 5 shows the photocatalytic degradation of MO and MV dyes by the UV/Cu^{2+}/PDS system. The results showed the enhancement in the percent degradation of MO and MV dyes by increasing the initial concentration of Cu^{2+} ions. The maximum percent degradation was achieved using 2.0 and 1.5 mM concentrations of Cu^{2+} for MO and MV dyes, respectively. At an irradiation time of 40 min, the percent degradation of these selected dyes with increases in the Cu^{2+} dosages from 0.5 to 1.0, 1.5, 2.0, 2.5 and 3.0 was 68.4, 79.3, 84.6, 94.0, 91.0 and 82.6% for MV and 62.7, 79.1, 89.0, 85.0, 83.0 and 77.6% for MO, respectively (Figure 5). The increase in the photocatalytic degradation of MO and MV is due to the fact that with photocatalytic activation of PDS by Cu^{2+} as shown by Equation (5) (Liang *et al.* 2013).

$$S_2O_8^{2-} + Cu^{2+} \rightarrow Cu^{3+} + SO_4^{\cdot-} + SO_4^{2-} \tag{5}$$

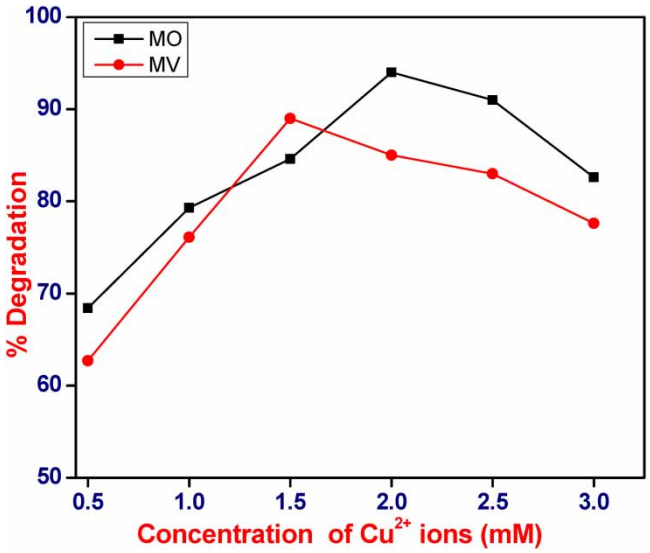

Figure 5 | Photocatalytic degradation of MO and MV using the UV/Cu^{2+}/PDS system. Experimental conditions: $[MO]_0 = 10$ ppm; $[MV]_0 = 25$ ppm; [PDS] = 1.5 mM; $[Cu^{2+}] = 0.5$–3 mM; radiation source = UV lamp (15 W); time = 40 min, $pH_{MO} = 4.5$, $pH_{MV} = 5.6$.

Downloaded from http://iwaponline.com/wpt/article-pdf/19/8/3317/1472464/wpt2024184.pdf
by guest

However, further increasing the initial concentration of Cu^{2+} beyond the optimum value (2 mM for MO and 1.5 mM for MV) showed a slight negative impact on the degradation of these contaminants. This could be associated with the limited PDS concentration at higher Cu^{2+} doses. These results are in agreement with the conclusions of Wang *et al.* (2020). Pasalari *et al.* (2022) also observed identical results where the excessive concentration of Cu^{2+} (25 mg L^{-1}) in the degradation performance of 2,4-dinitrophenol was reduced by the UV/PS/Cu^{2+} process. However, it is recommended to perform more research studies to explore exactly the role of Cu^{2+} at optimum concentrations.

3.4. Influence of initial pH of the solution on dye degradation

The photocatalytic efficiency of the UV/Cu^{2+}/PDS system toward MO and MV degradation was also determined at different pH media (3.0, 6.0 and 9.0), and the results are depicted in Figure 6. The natural solution pH of MO (pH_{MO}) and MV (pH_{MV}) was 4.5 and 5.6, respectively. It can be seen from Figure 6 that at an irradiation time of 40 min, the percent degradation of MO at pH = 3.0, 4.5, 6.0 and 9.0 was 82.0, 89.0, 94.0 and 79.0, respectively. Similarly, at an irradiation time of 40 min, the percent degradation of MV at pH =3.0, 5.6, 6.0 and 9.0 was 92.0, 94.0, 89.0 and 77.0%, respectively.

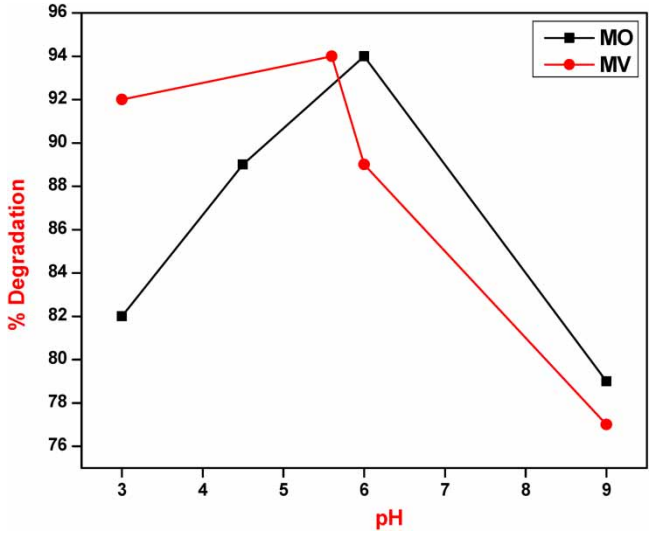

Figure 6 | Photocatalytic efficiency of the UV/Cu^{2+}/PDS systems toward MO and MV degradation in different pH media. Experimental conditions: [MO] = 10 ppm; [MV] = 25 ppm; [Cu^{2+}] = 2 mM; [PDS] = 1.5 mM; pH = 3, 6 and 9; radiation source = UV lamp (15 W); time = 40 min.

The results of Figure 6 indicate that the highest percent degradation of MO by the UV/Cu^{2+}/PDS system was achieved at a pH of 6.0. The free radical distribution in aqueous solution by PS activated system is such that at pH = 2–7 (acidic and neutral media) the main reactive species is $SO_4^{\cdot-}$, at pH = 8–10 both $^{\cdot}OH$ and $SO_4^{\cdot-}$ co-exists while at pH >10, OH is the dominant species (Li *et al.* 2014; Naz *et al.* 2024). Thus, with the rise in pH, $SO_4^{\cdot-}$ gradually converts to OH. Similarly, MO showed a higher percent photocatalytic degradation at pH = 5.6 by the UV/Cu^{2+}/PDS process. It also gives an indication that $SO_4^{\cdot-}$ is important for the effective photocatalytic degradation of MO and MV by the UV/Cu^{2+}/PDS process.

3.5. Photocatalytic degradation of MO and MV dyes in different water systems by UV/Cu^{2+}/PDS system

The photocatalytic efficiency of the UV/Cu^{2+}/PDS system toward MO and MV degradation was also determined in synthetic and IW samples besides the DW. The SW sample was prepared in the laboratory by the addition of various types of salts in aqueous media containing MO and MV dyes. The IW sample was collected from the Coca Cola plant. Prior to the treatment, the sample was contaminated with the known concentration of MO and MV dyes.

Downloaded from http://iwaponline.com/wpt/article-pdf/19/8/3317/1472464/wpt2024184.pdf
by guest

Figure 7 shows the photocatalytic degradation of MO and MV dyes in DW, SW and IW samples. Figure 7 revealed the enhanced degradation of MO (94%) and MV (89%) in DW compared to SW (MO = 74.7%, MV = 32.2%) and IW (MO = 75%, MV = 74%). The percent degradation of the UV/Cu^{2+}/PDS system in SW and IW compared to DW is due to the existence of various ionic species that act as scavengers for $^{\cdot}OH$ and $SO_4^{\cdot-}$ hence decreasing the percent degradation of MO and MV dyes (Equations 6–11) (Khan *et al.* 2023).

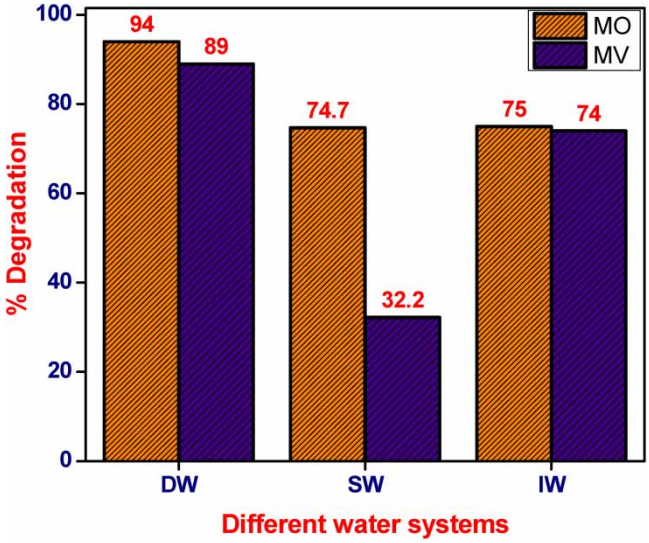

Figure 7 | Photocatalytic efficiency of the UV/Cu^{2+}/PDS system toward MO and MV degradation in water systems. Experimental conditions: [MO] = 10 ppm; [MV] = 25 ppm; [Cu^{2+}] = 2 mM; [PDS] = 1.5 mM; radiation source = UV lamp (15 W); time = 40 min, pH_{MO} = 4.5, pH_{MV} = 5.6.

$$^{\cdot}OH + CO_3^{2-} \rightarrow O_3^{\cdot-} + {}^{-}OH \quad (6)$$

$$SO_4^{\cdot-} + CO_3^{2-} \rightarrow CO_3^{\cdot-} + SO_4^{2-} \quad (7)$$

$$^{\cdot}OH + SO_4^{2-} \rightarrow SO_4^{\cdot-} + {}^{-}OH \quad (8)$$

$$SO_4^{\cdot-} + SO_4^{2-} \rightarrow S_2O_8^{2-} + e^{-} \quad (9)$$

$$^{\cdot}OH + Cl^{-} \rightarrow Cl_2^{\cdot-} + ClOH^{\cdot-} \quad (10)$$

$$SO_4^{\cdot-} + Cl^{-} \rightarrow Cl^{\cdot} + SO_4^{2-} \quad (11)$$

3.6. Mechanistic insight into the photocatalytic degradation of MO and MV dyes in the UV/Cu^{2+}/PDS system

To determine the investigate the mechanistic insights into the photocatalytic degradation of MO and MV dyes using the UV/Cu^{2+}/PDS system, the role of $^{\cdot}OH$ and $SO_4^{\cdot-}$ toward the MO and MV degradation is necessary to be determined first. In this regard, some scavenger experiments were carried out using isopropanol (tert-butanol) as a good scavenger of $^{\cdot}OH$ only (Gul *et al.* 2020), and ethanol as both $^{\cdot}OH$ and $SO_4^{\cdot-}$ scavenger (Khan *et al.* 2023). The results of the scavenger experiments are depicted in Figure 8. Figure 8 shows that, upon the introduction of radical species in the saturated media containing the MO and MV dyes, a decrease in percent degradation was observed. At an irradiation time of 40 min, the percent degradation of MO was decreased from 94.0% (without scavenger) to 78.0% in the case of isopropanol and to 32.6% in the case of ethanol. Similarly, at an irradiation time of 40 min, the percent degradation of MV was decreased from 89.0% (without scavenger) to 76.0% in the case of isopropanol and to 42.0% in the case of ethanol. The results indicate that the lowest photocatalytic efficiency of the UV/Cu^{2+}/PDS system toward MO and MV dyes was observed when the solution is added with ethanol, which is a good scavenger of both $^{\cdot}OH$ and $SO_4^{\cdot-}$. Thus, the scavenger experiments revealed $SO_4^{\cdot-}$ as the prominent species responsible for MO and MV degradation.

Downloaded from http://iwaponline.com/wpt/article-pdf/19/8/3317/1472464/wpt2024184.pdf
by guest

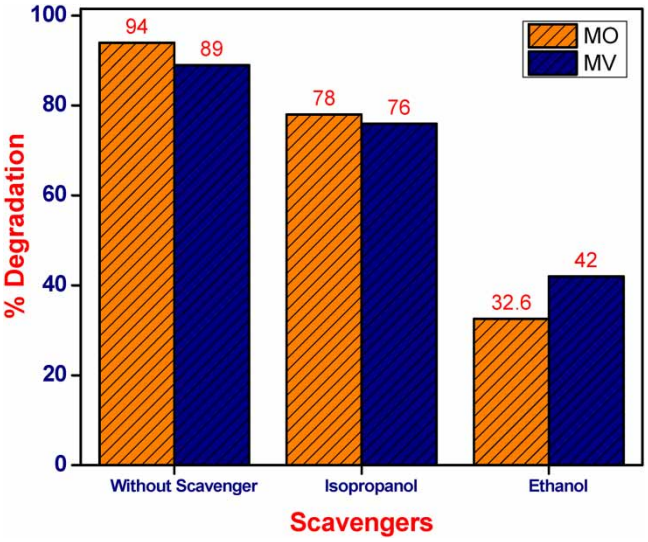

Figure 8 | Effects of radical scavengers in MO and MV degradation in the UV/Cu^{2+}/PDS system. Experimental conditions: [MO] = 10 ppm; [MV] = 25 ppm; [Cu^{2+}] = 2 mM; [PDS] = 1.5 mM; [Tert-Butanol] = 2 mM; [Isopropanol] = 2 mM; [Ethanol] = 2 mM; radiation source = UV lamp (15 W); time = 40 min, pH_{MO} = 4.5, pH_{MV} = 5.6.

In the light of the above discussions, PDS in the presence of UV-254 nm radiation when reacts with Cu^{2+} as a catalyst results in the formation of Cu^{3+} and $SO_4^{\cdot-}$ (Equation (5)). In this system, Cu^{2+} plays a synergistic role in the photocatalytic activation of PDS to form $SO_4^{\cdot-}$. The generated $SO_4^{\cdot-}$ then attacked the MO and MV dyes and caused their destruction in reaction media. The overall schematic representation of the UV/Cu^{2+}/PDS system is depicted in Figure 9.

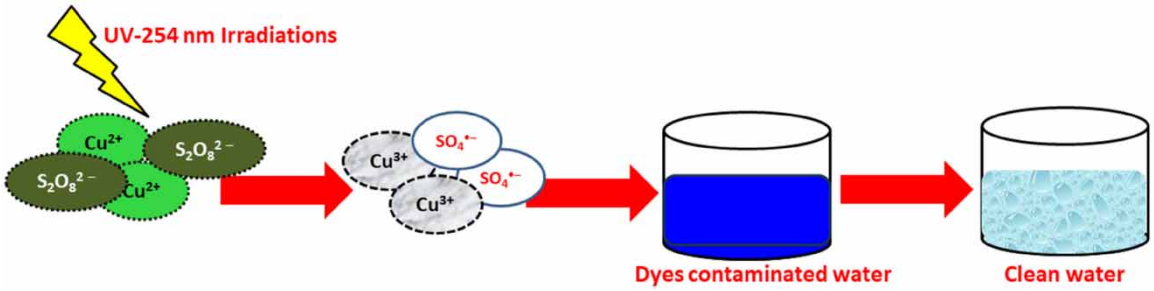

Figure 9 | Proposed mechanism of activation of the UV/Cu^{2+}/PDS system for degradation of MO and MV dyes.

3.7. Identification of degradation by-products and development of possible degradation pathways

The respective solutions of MO and MV dyes after treatment in the UV/Cu^{2+}/PDS system were analyzed by GC-MS. The GC-MS analysis revealed that various DPs results from the degradation of MO and MV dyes. The structures of these DPs were obtained from their chemical formulae and *m/z* values.

The molecular formula and *m/z* value for azo-anionic MO dye is $C_{14}H_{14}N_3NaO_3S$ and 304, respectively. The formation of DP1 in Figure 10, *m/z* 261, resulted from the de-amination of MO dye. Direct photolysis and $^{\cdot}OH/SO_4^{\cdot-}$ could possibly contribute to this by-product. The formation of DP2, *m/z* 229, resulted from DP1 in which SO_3 was further reduced to SO. DP3, *m/z* 186, resulted from DP1 on the removal of the aromatic ring by complex reaction. DP4, *m/z* 173, had resulted from DP3 by oxidation by $^{\cdot}OH$. DP5, *m/z* 171, had also resulted from DP3 by removal of the amine group and addition of methyl group at the ortho position. DP6, *m/z* 157, resulted either from DP4 by dehydroxylation or DP5 by demethylation, and no further attack of radicals was shown. DP7, *m/z* 59, was the simplest by-product resulting from side reactions.

Downloaded from http://iwaponline.com/wpt/article-pdf/19/8/3317/1472464/wpt2024184.pdf
by guest

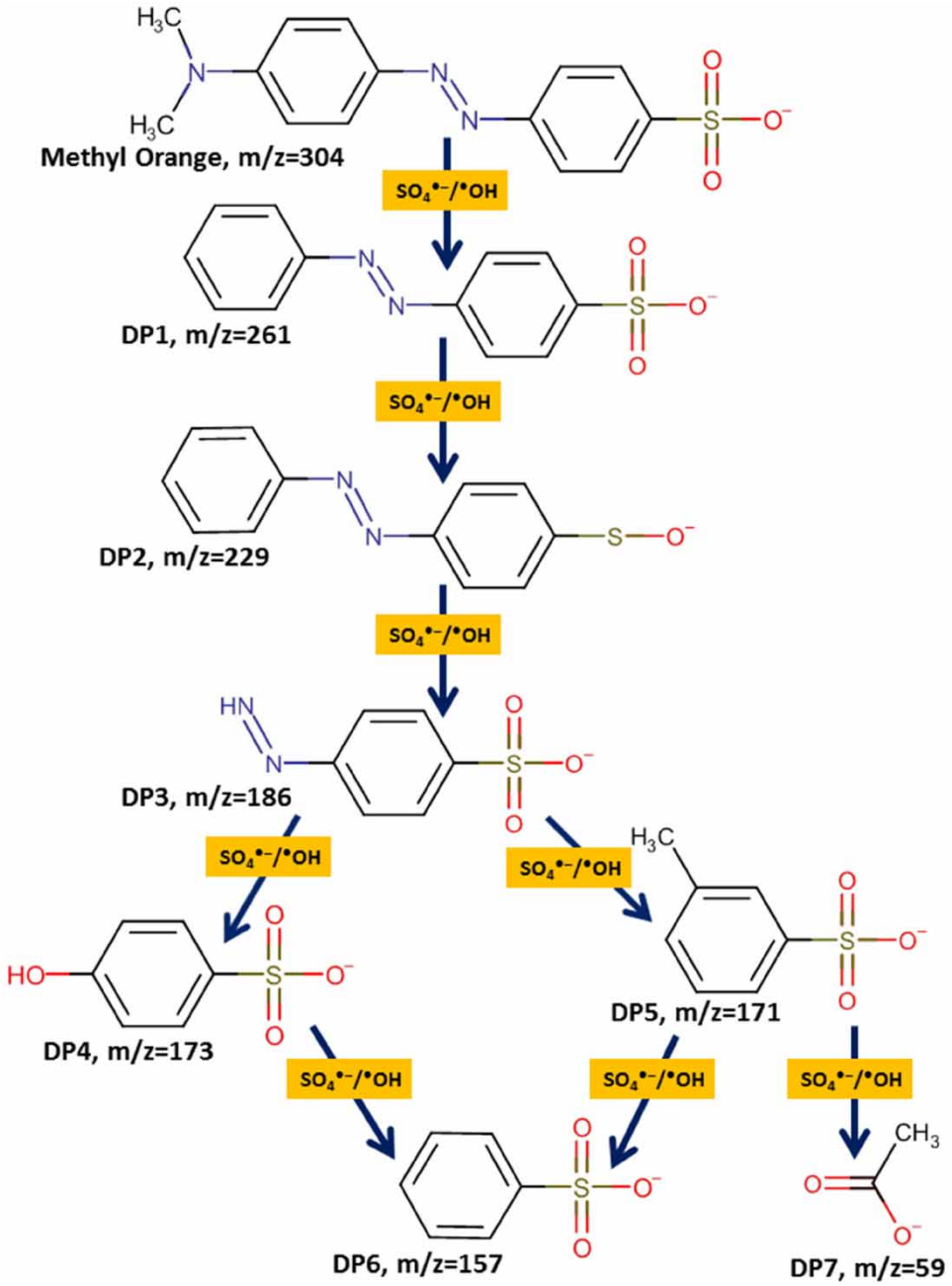

Figure 10 | Degradation pathway for MO dye in the UV/Cu^{2+}/PDS system.

The molecular formula and *m/z* value for cationic MV dye are $C_{24}H_{28}N_3Cl$ and 358, respectively. Figure 11 shows that DP1, *m/z* 281, resulted from the reduction of MV dye. Direct photolysis and $^{\cdot}OH/SO_4^{\cdot-}$ could possibly contribute to this by-product. DP2, *m/z* 220, was formed by the reduction in which amine groups are eliminated. DP3, *m/z* 211, resulted from the removal of the aromatic ring and amine group by complex reaction. DP4, *m/z* 183, had resulted from DP3 by reduction through OH. DP5, *m/z* 135, had also resulted from DP3 by splitting under UV irradiations. DP6, *m/z* 59, and DP7, *m/z* 45, were the simplest by-products that resulted from complex oxidation reduction reactions.

4. CONCLUSIONS

The photocatalytic degradation of MO and MV dyes by the UV/Cu^{2+}/PDS system showed promising results. The results indicated that the photocatalytic degradation of MO (10 ppm) and MV (25 ppm) was optimized at Cu^{2+}

Downloaded from http://iwaponline.com/wpt/article-pdf/19/8/3317/1472464/wpt2024184.pdf
by guest

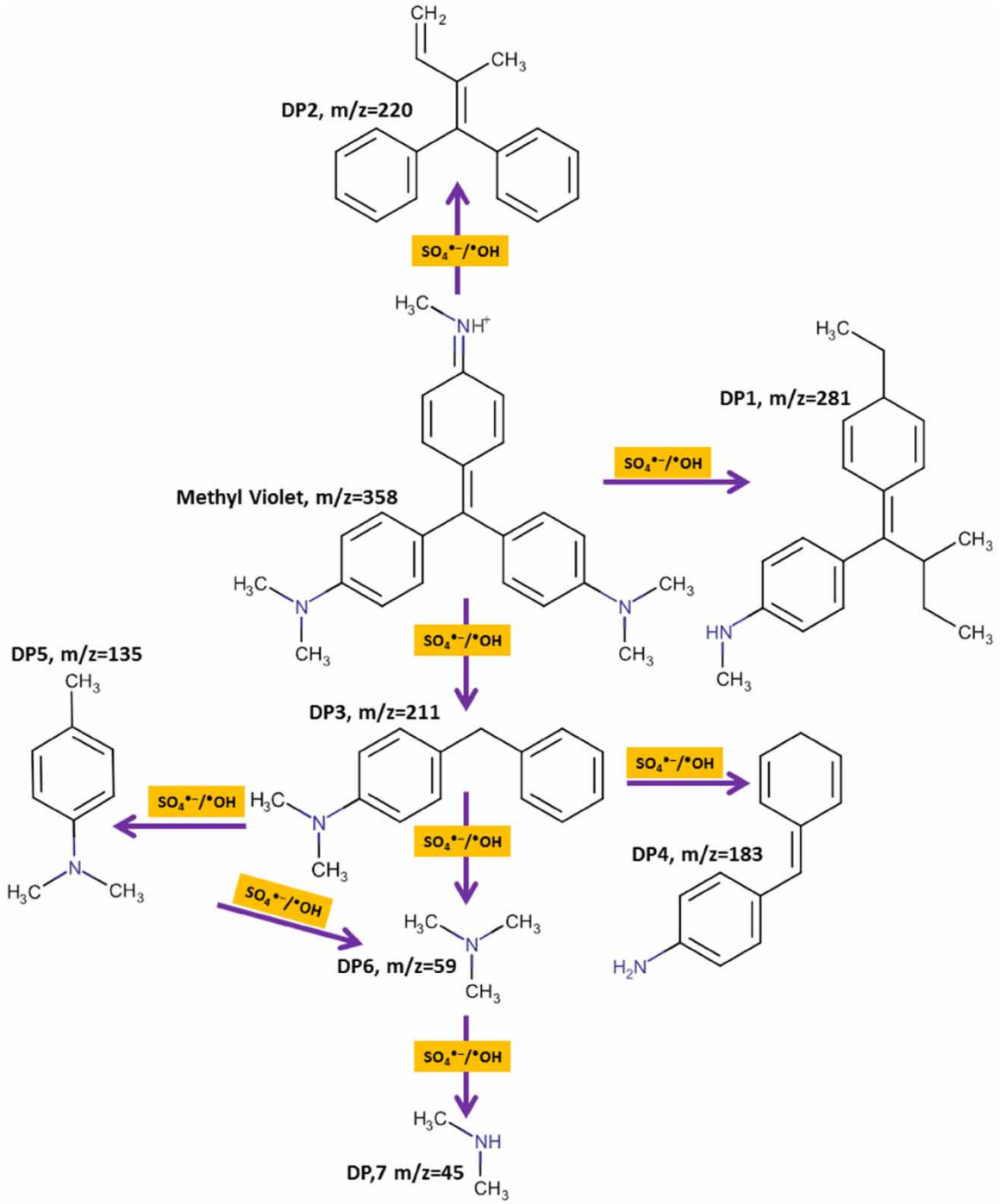

Figure 11 | Degradation pathway for MV in the UV/Cu^{2+}/PDS system.

and PDS having concentrations of 2 and 1.5 mM, respectively. The maximum photocatalytic degradation of MV was achieved at pH = 3.0, while for MO, it was 6.0. The scavenger studies indicated that $SO_4^{\bullet-}$ is the dominant species involved in the photocatalytic degradation of MO and MV. The results from different water types (DW, IW, SW) showed that despite the quality of water, the UV/Cu^{2+}/PDS process is the best environmentally friendly and effective treatment technology for the degradation of MO and MV dyes in water.

ACKNOWLEDGEMENTS

The authors acknowledge the Higher Education Commission (HEC) of Pakistan for providing financial support to this work through project No. 17212.

Downloaded from http://iwaponline.com/wpt/article-pdf/19/8/3317/1472464/wpt2024184.pdf
by guest

AUTHOR CONTRIBUTIONS

The individual contributions of all the authors to this paper can be summarized as follows: QK contributed to conceptualization, data curation, formal analysis, Investigation, methodology, and writing the original draft. AA contributed to formal analysis, investigation, validation, and editing. MS contributed to project administration, supervision, and funding acquisition. IG contributed to validation and editing. FG contributed to revising the manuscript. FR contributed in revising and editing the manuscript. MZ contributed to revising the manuscript.

DATA AVAILABILITY STATEMENT

All relevant data are included in the paper or its Supplementary Information.

CONFLICT OF INTEREST

The authors declare there is no conflict.

REFERENCES

Al-Mamun, M. R., Kader, S. & Islam, M. S. 2021 Solar-TiO_2 immobilized photocatalytic reactors performance assessment in the degradation of methyl orange dye in aqueous solution. *Environmental Nanotechnology, Monitoring & Management* **16**, 100514.

Artagan, Ö., Vaizoğullar, A. İ. & Uğurlu, M. 2021 Activated carbon-supported NiS/CoS photocatalyst for degradation of methyl violet (MV) and selective disinfection process for different bacteria under visible light irradiation. *Journal of Taibah University for Science* **15**(1), 154–169.

Badi, M. Y., Esrafili, A., Pasalari, H., Kalantary, R. R., Ahmadi, E., Gholami, M. & Azari, A. 2019 Degradation of dimethyl phthalate using persulfate activated by UV and ferrous ions: Optimizing operational parameters mechanism and pathway. *Journal of Environmental Health Science Engineering* **17**, 685–700.

Bekkouche, S., Merouani, S., Hamdaoui, O. & Bouhelassa, M. 2017 Efficient photocatalytic degradation of safranin O by integrating solar-UV/TiO_2/persulfate treatment: Implication of sulfate radical in the oxidation process and effect of various water matrix components. *Journal of Photochemistry Photobiology A: Chemistry* **345**, 80–91.

Bougdour, N., Tiskatine, R., Bakas, I. & Assabbane, A. 2020 Textile wastewater treatment by peroxydisulfate/Fe (II)/UV: Operating cost evaluation and phytotoxicity studies. *Chemistry Africa* **3**, 153–160.

Chakma, S., Praneeth, S. & Moholkar, V. S. 2017 Mechanistic investigations in sono-hybrid (ultrasound/Fe2+/UVC) techniques of persulfate activation for degradation of azorubine. *Ultrasonics Sonochemistry* **38**, 652–663.

El-Regal, M. A. & Satheesh, S. 2023 Biodiversity of marine ecosystems. *Marine Ecosystems: A Unique Source of Valuable Bioactive Compounds* **3**, 1–42.

Gokulakrishnan, S., Parakh, P. & Prakash, H. 2013 Photodegradation of methyl orange and photoinactivation of bacteria by visible light activation of persulphate using a tris (2, 20-bipyridyl) ruthenium (II) complex. *Journal of Photochemical & Photobiological Sciences* **12**(3), 456.

Gul, I., Sayed, M., Shah, N. S., Khan, J. A., Polychronopoulou, K., Iqbal, J. & Rehman, F. 2020 Solar light responsive bismuth doped titania with Ti^{3+} for efficient photocatalytic degradation of flumequine: Synergistic role of peroxymonosulfate. *Chemical Engineering Journal* **384**, 123255.

Inyinbor Adejumoke, A., Adebesin Babatunde, O., Oluyori Abimbola, P., Adelani Akande Tabitha, A., Dada Adewumi, O. & Oreofe Toyin, A. 2018 Water pollution: Effects, prevention, and climatic impact. *Water Challenges of an Urbanizing World* **33**, 33–47.

Ismail, G. A. & Sakai, H. 2022 Review on effect of different type of dyes on advanced oxidation processes (AOPs) for textile color removal. *Chemosphere* **291**, 132906.

Keskin, M. S., Horoz, S., Şahin, Ö. & Kutluay, S. 2024 Development of Al_2O_3-supported nanobimetallic Co-La-B catalyst for boosting hydrogen release via sodium borohydride hydrolysis. *Journal of the Australian Ceramic Society* 1–11.

Khan, Q., Sayed, M. & Gul, I. 2023 Titania/reduced graphene oxide nanocomposites (TiO_2/rGO) as an efficient photocatalyst for the effective degradation of brilliant green in aqueous media: Effect of peroxymonosulfate and operational parameters. *Environmental Science and Pollution Research* **30**(27), 71025–71047.

Khan, Q., Sayed, M., Khan, J. A., Rehman, F., Noreen, S., Sohni, S. & Gul, I. 2024 Advanced oxidation/reduction processes (AO/RPs) for wastewater treatment, current challenges, and future perspectives: A review. *Environmental Science Pollution Research* **31**(2), 1863–1889.

Kuchangi, S. N., Mruthunjayappa, M. H. & Kotrappanavar, N. S. 2023 An overview of water pollutants in present scenario. In: *3D Printing Technology for Water Treatment Applications* (Pandey, J. K., Manna, S. & Patel, R. K., eds.). pp. 83–105. https://doi.org/10.1016/C2021-0-00162-0.

Li, H., Guo, J., Yang, L. & Lan, Y. 2014 Degradation of methyl orange by sodium persulfate activated with zero-valent zinc. *Separation Purification Technology* **132**, 168–173.

Downloaded from http://iwaponline.com/wpt/article-pdf/19/8/3317/1472464/wpt2024184.pdf
by guest

Liang, H.-y., Zhang, Y.-q., Huang, S.-b. & Hussain, I. 2013 Oxidative degradation of p-chloroaniline by copper oxidate activated persulfate. *Chemical Engineering Journal* **218**, 384–391.

Liu, H., Liu, F., Zhang, J., Zhou, J., Bi, W., Qin, J., Hou, Q., Ni, Y., Xu, S. & Yang, C. 2022 Degradation of methyl orange by pyrite activated persulfate oxidation: Mechanism, pathway and influences of water substrates. *Water Science Technology* **85**(10), 2912–2927.

Liu, B., Huang, B., Wang, Z., Tang, L., Ji, C., Zhao, C., Feng, L. & Feng, Y. 2023a Homogeneous/heterogeneous metal-catalyzed persulfate oxidation technology for organic pollutants elimination: A review. *Journal of Environmental Chemical Engineering* **11**(3), 109586.

Liu, W., Lu, Y., Dong, Y., Jin, Q. & Lin, H. 2023b A critical review on reliability of quenching experiment in advanced oxidation processes. *Chemical Engineering Journal* **466**, 143161.

Naz, K., Sayed, M., Rehman, F., Gul, I., Noreen, S., Khan, Q., Gul, S. & Hussain, S. 2024 Photochemical degradation of bromocresol green dye by UV/Co^{2+} process via activation of peroxymonosulfate: A mechanistic approach. *Water Practice Technology* **19**(3), 1003–1015.

Nidheesh, P. V., Divyapriya, G., Titchou, F. E. & Hamdani, M. 2022 Treatment of textile wastewater by sulfate radical based advanced oxidation processes. *Separation and Purification Technology* **293**, 121115.

Orak, C. & Yüksel, A. 2021 Photocatalytic hydrogen energy evolution from sugar beet wastewater. *ChemistrySelect* **6**(43), 12266–12275.

Orak, C. & Yüksel, A. 2022a Comparison of photocatalytic performances of solar-driven hybrid catalysts for hydrogen energy evolution from 1, 8–diazabicyclo [5.4. 0] undec-7-ene (DBU) solution. *International Journal of Hydrogen Energy* **47**(14), 8841–8857.

Orak, C. & Yüksel, A. 2022b Box–Behnken design for hydrogen evolution from sugar industry wastewater using solar-driven hybrid catalysts. *ACS Omega* **7**(46), 42489–42498.

Pasalari, H., Esrafili, A., Yegane Badi, M. & Farzadkia, M. 2022 Degradation of 2, 4-dinitrophenol using persulfate activated by Cu^{2+} in photocatalytic system (UV/SPS/Cu^{2+}) from aqueous solution: Optimisation and operational parameters. *International Journal of Environmental Analytical Chemistry* **102**(3), 804–819.

Rehman, F., Sayed, M., Khan, J. A., Shah, N. S., Khan, H. M. & Dionysiou, D. D. 2018 Oxidative removal of brilliant green by UV/$S_2O_8^{2-}$, UV/HSO_5–and UV/H_2O_2 processes in aqueous media: A comparative study. *Journal of Hazardous Materials* **357**, 506–514.

Shah, R. K. 2023 Efficient photocatalytic degradation of methyl orange dye using facilely synthesized α-Fe_2O_3 nanoparticles. *Arabian Journal of Chemistry* **16**(2), 104444.

Sidabutar, N., Namara, I., Hartono, D. & Soesilo, T. 2017. The effect of anthropogenic activities to the decrease of water quality. In: *IOP Conference Series: Earth and Environmental Science*, IOP Publishing, p. 012034.

Thekkedath, A., Sugaraj, S. & Sridharan, K. 2022 Nanomaterials in advanced oxidation processes (AOPs) in anionic dye removal. In: *Advanced Oxidation Processes in Dye-Containing Wastewater* (Muthu, S. S. & Khadir, A. eds.). Vol. 1, Springer, Singapore. pp. 129–165.

Tian, D., Zhou, H., Zhang, H., Zhou, P., You, J., Yao, G., Pan, Z., Liu, Y. & Lai, B. 2022 Heterogeneous photocatalyst-driven persulfate activation process under visible light irradiation: From basic catalyst design principles to novel enhancement strategies. *Chemical Engineering Journal* **428**, 131166.

Wang, B., Fu, T., An, B. & Liu, Y. 2020 UV light-assisted persulfate activation by Cu^0-Cu_2O for the degradation of sulfamerazine. *Separation Purification Technology* **251**, 117321.

Zaharia, C., Suteu, D., Muresan, A., Muresan, R. & Popescu, A. 2009 Textile wastewater treatment by homogenous oxidation with hydrogen peroxide. *Environmental Engineering and Management Journal* **8**(6), 1359–1369.

Zhang, T., Chen, Y., Wang, Y., Le Roux, J., Yang, Y. & Croué, J.-P. 2014 Efficient peroxydisulfate activation process not relying on sulfate radical generation for water pollutant degradation. *Environmental Science & Technology* **48**(10), 5868–5875.

Zhang, L., Xiao, C., Li, Z., Guo, J., Du, G., Cheng, X. & Jia, Y. 2023 Degradation of methyl orange using persulfate activated by magnetic CuS/Fe_3O_4 catalyst: Catalytic performance and mechanisms. *Applied Surface Science* **618**, 156595.

Zohaib, M., Sayed, M., Rehman, F., Gul, S., Noreen, S., Sohni, S., Gul, I. & Ali, A. 2024 Synthesis and characterization of zero valent iron/Cellulose acetate (Fe0-x/CA) membranes for the catalytic degradation of methylene blue from aqueous media by activating peroxymonosulfate. *Catalysis Surveys From Asia* 1–15.

First received 18 March 2024; accepted in revised form 1 July 2024. Available online 15 July 2024

Downloaded from http://iwaponline.com/wpt/article-pdf/19/8/3317/1472464/wpt2024184.pdf
by guest